HHS Public Access

Author manuscript

Mol Cancer Res. Author manuscript; available in PMC 2018 December 01.

Published in final edited form as:

Mol Cancer Res. 2017 December ; 15(12): 1733–1740. doi:10.1158/1541-7786.MCR-17-0315.

The Influential Role of BCL2 Family Members in Synovial Sarcomagenesis

Jared J. Barrott[1,2,3], **Ju-Fen Zhu**[1,2,3], **Kyllie Smith-Fry**[1,2,3], **Asia M. Susko**[1,2,3], **Dakota Nollner**[1,2,3], **Lance D. Burrell**[3,5], **Amir Pozner**[4], **Mario R. Capecchi**[4], **Jeffrey T. Yap**[3,5,6], **Lisa A. Cannon-Albright**[3,7], **Xingming Deng**[8], and **Kevin B. Jones**[1,2,3]

[1]Department of Orthopaedics, University of Utah School of Medicine, Salt Lake City, Utah

[2]Department of Oncological Sciences, University of Utah School of Medicine, Salt Lake City, Utah

[3]Huntsman Cancer Institute, University of Utah School of Medicine, Salt Lake City, Utah

[4]Department of Human Genetics, University of Utah School of Medicine, Salt Lake City, Utah

[5]Center for Quantitative Cancer Imaging, University of Utah School of Medicine, Salt Lake City, Utah

[6]Department of Radiology and Imaging Sciences, University of Utah School of Medicine, Salt Lake City, Utah

[7]Department of Genetic Epidemiology, University of Utah School of Medicine, Salt Lake City, Utah

[8]Department of Radiation Oncology, Emory University School of Medicine, Atlanta, Georgia

Abstract

Synovial sarcomas are deadly soft-tissue malignancies associated with t(X;18) balanced chromosomal translocations. Expression of the apoptotic regulator BCL2 is prominent in synovial sarcomas and has prompted the hypothesis that synovial sarcomagenesis may depend on it. Herein, it is demonstrated that *Bcl2* overexpression enhances synovial sarcomagenesis in an animal model. Further, we determined increased familial clustering of human synovial sarcoma patients with victims of other BCL2-associated malignancies in the Utah Population Database. Conditional genetic disruption of *Bcl2* in mice also led to reduced sarcomagenesis. Pharmacologic inhibition specific to BCL2 had no demonstrable efficacy against human synovial sarcoma cell lines or mouse tumors. However, targeting BCLxL in human and mouse synovial sarcoma with the small molecule BH3 domain inhibitor, BXI-72, achieved significant cytoreduction and increased apoptotic signaling. Thus, the contributory role of BCL2 in synovial sarcomagenesis does not

Contact: Kevin B. Jones, MD, Primary Children's and Families' Cancer Research Center, Huntsman Cancer Institute, University of Utah School of Medicine, 2000 Circle of Hope Drive, Research South 3726, Salt Lake City, Utah 84112, (e) kevin.jones@hci.utah.edu, (v) 801-585-0300, (f) 801-585-7084.

Conflict of Interest: The authors declare no conflict of interest with the material presented.

Author contributions

JJB and KJB conceived the idea, designed experiments, and wrote the manuscript. JJB, JFZ, HJ, KSF, AMS, DN carried out experimental plans. XD provided the compound BXI-72 and expertise in dosing. JY, LB designed, acquired, and analyzed FDG-PET/CT images. LCA conducted analyses using the UPDB. All authors reviewed and edited the manuscript.

appear to render it as a therapeutic target, but mitrochondrial anti-apoptotic BCL2 family members may be.

Keywords

Mouse model; synovial sarcoma; BCL2 family members; apoptosis

Introduction

Synovial sarcoma (SS) is a deadly soft-tissue malignancy (1). Almost half of SS patients develop metastasis by 5 years (2), and thus become practically incurable. The current systemic therapy armamentarium consists primarily of traditional cytotoxic chemotherapies, which demonstrate only limited ultimate effectiveness (3, 4). The chromosomal translocation *t(X;18)* generating a fusion oncogene, *SS18-SSX1, SS18-SSX2*, or *SS18-SSX4*, is the characteristic feature and driving genomic alteration responsible for SS (5). SS18-SSX oncoproteins have been shown to misregulate BAF complexes in chromatin remodeling as well as recruiting repressive polycomb group complexes to ATF2-bound loci (6, 7).

BCL2 is prominently expressed in SS (8). Strong immunohistochemical staining of BCL2 was considered a diagnostic feature for SS before molecular evidence of the translocation became testable in clinical laboratories (8). We have previously shown that *Bcl2* is upregulated in embryonic fibroblasts by the exogenous addition of *SS18-SSX2* and reduced in SS cell lines by the introduction of siRNAs against *SS18-SSX2* (9), leading some to postulate that BCL2 could be a therapeutic target in SS.

The *Bcl2* family consists of 25 gene products that regulate mitochondrial apoptosis, with both pro-apoptotic and anti-apoptotic members (10). Both pro- and anti-apoptotic members of the BCL2 family are relatively upregulated in SS (9). However, we previously observed that transcription of certain anti-apoptotic genes in the family, namely MCL1 and BCL2A1 were specifically suppressed by the action of the fusion oncoprotein (9). Navitoclax (ABT-263), an inhibitor of the remaining anti-apoptotic family members, BCL2 itself, BCLxL and BCLw, was demonstrated to have some efficacy against human SS cell lines and in the mouse genetic model of SS, as a single agent, or synergistically with doxorubicin (9). However, navitoclax stalled in its early clinical development due to toxicity manifest by thrombocytopenia (11). More BCL2-specific BH-domain peptidomimetics have been shown to avoid the dangerous megakaryocyte suppression. One such compound, Venetoclax (RG7601, GDC-0199/ABT-199), has just received breakthrough therapy designation for relapsed or refractory chronic lymphocytic leukemia with 17p deletion (12, 13). Inhibitors of other family members have also been developed. BXI-72 is a novel BCLxL inhibitor that selectively disrupts its interactions with BAK and BAX, thus allowing cytochrome c release from the mitochondria. Additionally, BXI-72 has shown efficacy in *in vivo* lung cancer models (14). We determined to interrogate BCL2 with regard to its role in synovial sarcomagenesis, as well as the pathway's potential druggability with newer agents.

Materials and Methods

Utah Population Methods

The Utah Population DataBase (UPDB) is a computerized genealogy of the Utah pioneer founders from the mid 1800s to modern day. The genealogy data is linked to the Utah Cancer Registry, which has recorded all cancers diagnosed or treated in Utah from 1966, and became a statewide NCI Surveillance, Epidemiology, and End-Results (SEER) Registry in 1973. Almost 3 million individuals in the UPDB have at least 3 generations of genealogy data, including approximately 150,000 individuals with a cancer diagnosis; 68 of them diagnosed with synovial sarcoma (defined as histology 9040–9043 from the International Classification for Oncology Revision 3. BCL2-related malignancies considered included: non-Hodgkin's lymphomas, acute myeloid leukemias, chronic myeloid leukemias, and myelodysplastic syndromes.

The relative risk for BCL2-associated cancers in each set of relatives was estimated as the observed number of cancers divided by the expected number of cancers. All individuals in UPDB with at least 3 generations of genealogy were assigned to a cohort based on sex, 5 year birth year range, and birth place (Utah or other), and cohort-specific BCL2-associated cancer rates were estimated as the total number of BCL2 cancers divided by the total number of individuals in each cohort. To estimate the expected number of BCL2 cancer cases in each group of relatives, all relatives were counted by cohort (without duplication), the number of relatives in each cohort was multiplied by the cohort-specific rate of BCL2 cancers, and the expected numbers were summed over all cohorts. The distribution of the number of observed cancer cases is assumed to be Poisson with a mean equal to the expected number of cancers; 95% confidence intervals for RR were calculated as presented in Agresti et al. (15).

Mice

Mouse experiments were conducted with the approval of the institutional animal care committee in accordance with legal and ethical standards (protocol # 14-01016). The previously described, *Myf5Cre;Rosa26*^{hSS2}*Hprt-LSL-Bcl2, Bcl2*$^{fl/fl}$, and *Pten*$^{fl/fl}$*;hSS2* mice were maintained on a mixed strain background, C57BL/6 and SvJ. Genotyping primer sequences are in Supplementary Table 1. TATCre injections were 10 μL at 42 μM at 30 days of age. Radiographs were obtained with a Kodak Carestream 4000ProFx (Carestream Health, Inc., Rochester, NY, USA) and light photomicrographs with an Olympus BX43 microscope and DP26 camera (Olympus America, Center Valley, PA, USA). Also a 3.5X-90X LED low heat zoom stereo microscope equipped with 5MP digital camera was used to image gross tumors (Amscope, Irvine, CA, USA). *hSS2;Pten*$^{fl/fl}$ mice were treated with 20 mg/kg of BXI-72 in 10% DMSO/PBS or vehicle by IP once daily for 7 days. Mice were also treated 3 weeks with 100 mg/kg ABT-199 in 10% ethanol/30% PEG400/60% Ph50PG by oral gavage, control solution 10% ethanol/30% PEG400/60% Ph50PG by oral gavage, or weekly IV injections of 30 mg/kg doxorubicin (0.6 mg/mL in sterile saline). Bi-dimensional measurements were taken with digital calipers for both length and width and volume was calculated using the following equation: volume = length × width^2/2.

FDG-PET/CT imaging was performed using an Inveon™ small animal PET/CT scanner (Siemens Medical Solutions, Knoxville, TN). Mice were fasted overnight prior to imaging sessions. Animals were induced for anesthesia at 4–5% sevoflurane and 1.5 LPM oxygen and anesthesia maintained at 2–4% during the 60 minute uptake. Mice were injected with 0.3–0.5 mCi of FDG. A 20 minute PET emission scan was performed at ~60 minutes following the FDG injection with the CT scan performed immediately prior to the PET scan. Images were reconstructed with 3D-MAP/OSEM iterative reconstruction and corrected for decay, random coincidences, and attenuation. Parametric images of the Standardize Uptake Value (SUV) were generated by normalizing for injected FDG activity and animal weight. Image analysis was performed using VivoQuant™ (inviCRO, Boston, MA). Semi-automated metabolic tumor volumes were defined using connected threshold segmentation and the Total Lesion Glycolysis (TLG) was calculated as the metabolic tumor volume multiplied by the mean SUV.

Histology

Tissues were fixed in 4% paraformaldehyde overnight, and embedded in paraffin. Paraffin-embedded tissues were stained by hematoxylin and eosin.

Cell Lines

The human SYO-1 (16), Fuji (17), Aska and Yamato (18) cell lines, were received from Torsten Nielsen at the University of British Columbia. MoJoSS was developed as previous described from a consented patient's synovial sarcoma (19)]. Each was maintained in Dulbecco's modified eagle medium (DMEM) with 10% fetal bovine serum (FBS) and tested for mycoplasma using MycoAlert Plus (Lonza, Walkersville, MD) every 6 months. Cells treated with ABT-199, BXI-72, doxorubicin or control were incubated for 48 hours post treatment and assayed for viability using CellTitreGlo.

Synergy experiments were performed using the general MacSynergy protocol. In brief, 5,000 cells were seeded in a 96-well plate and after 24 hours were treated with serial dilutions of compounds in combination with doxorubicin. After 72 hours, cell viability was determined using CellTiter-Glo. Use the 99%CI graph and accompanying synergy/antagonism values for presentations. Rough estimates of significance for absolute values of synergy volumes (uM^2%): 0–25 (none), 25–50 (low), 50–100 (moderate), 100+ (high).

Immunoblotting

Protein was isolated from cells or tissues by incubating in a mild lysis buffer (10 mM Tris-HCl pH 8.1, 10 mM NaCl, 0.5% NP-40, and proteinase inhibitors). The fractions were clarified at 14,000 rpm for 10 min before loading 25 μg/sample for gel electrophoresis and transfer to PVDF membrane. Western blots were probed with the following primary antibodies: anti- BCLxL (Abcam, ab178844), anti-BID (Abcam, ab62469) anti-GAPDH (Millipore, MAB374) and anti-tubulin (Sigma Aldrich, T9026) and probed secondarily with goat anti-rabbit or goat anti-mouse antibodies conjugated with horse radish peroxidase and bands were detected using Bio-Rad Gel Doc MP imaging station.

qPCR detection

Tumor DNA was harvested using DNeasy tissue and blood kit (Qiagen). Quantitative PCR used the PerfeCTa SYBR Green FastMix (Quanta Biosciences) and a CFX Connect (Bio-Rad Laboratories) for detection using the following primer sequences: 3'UTR nPCR sense - ACACGCTAACATGGTTGTGC; anti-sense – TTCATGCCTTGTCTCCCAGG. Floxed detection dPCR sense – GCCCACCATCTAAAGAGCAA; anti-sense – GCATTTTCCCACCACTGTCT.

Statistical Methods

For most comparisons between sarcomas a two-tailed student's T-test was performed. All sample sizes are stated in the figure legends unless each data point is plotted in the figure. Statistical significance for the Kaplan Meier plots was determined by using a Log-rank test. Synergy was determined using the MacSynergy II software (20).

Results

Overexpression of *Bcl2* enhances synovial sarcomagenesis

To examine whether enhanced levels of expression of BCL2 in a mouse model of SS could enhance sarcomagenesis, we developed a mouse allele with conditional overexpression of *Bcl2* from a *CAGG* promoter, targeted to the *Hprt* locus ($Bcl2^{OE}$) (Fig. 1A). We crossed $Bcl2^{OE}$ mice with *Rosa26-LSL-SS18-SSX2* (*hSS2*) mice and conditionally induced recombination and expression from both alleles by injecting limbs with the TATCre protein (Fig. 1B). 7 of 9 injections led to tumorigenesis by age 9 months (Fig. 1C). TATCre injection into *hSS2* mice without additional BCL2 overexpression had a median time to tumorigenesis of 18.8 months in 18 of 37 mice. The H&E histology and IHC staining of these TATCre +$hSS2;Bcl2^{OE}$ mice did not deviate from typical SS patterns, including the development of both monophasic and biphasic histomorphology (the latter pathognomonic for SS and consisting of both mesenchymal spindled cells and others looking more epithelial and even forming mucinous gland-like structures) (Fig. 1D).

Upon activating $Bcl2^{OE}$ and *hSS2* in the *Myf5* lineage (Fig. 1E), we observed a 3-week earlier onset to sarcomagenesis compared to SS18-SSX2 expression alone (z-score 2.28, p=0.023) (Fig. 1F). Again, histology and immunohistochemistry shared characteristics with human SS and other mouse models of SS (Fig. 1G–H).

SS associates with other BCL2-driven malignancies in families, suggesting subtle heritable predisposition

To test the association of SS with a predisposition toward increased BCL2 expression in a human population, we turned to the Utah Population Database (UPDB). We tested 1st-, 2nd-, and 3rd-degree relatives of synovial sarcomas for an excess of BCL2-linked cancers such as follicular lymphoma and chronic lymphocytic leukemia. A significant excess of BCL2-related malignancies was observed among second-degree relatives of synovial sarcoma cases (p=0.007), and borderline significant excesses were observed in first-degree (p=0.087) and third-degree (p=0.051) suggesting inherited risk for synovial sarcoma is associated with Bcl2 overexpression (Table 1).

Genetic disruption of *Bcl2* inhibits synovial sarcomagenesis

Conditional activation of the *hSS2* allele by *Myf5Cre* has been shown to have a nearly completely penetrant phenotype of synovial sarcomagenesis. We bred *hSS2* mice to $Bcl2^{fl/fl}$ mice to generate combined expression of SS18-SSX2 and loss of BCL2 (Fig. 2A–B). Compared to *hSS2* alone, mice with added homozygosity for conditional disruption of *Bcl2* still formed morbid tumors, but at a slightly delayed time-frame and slightly smaller number of tumors per mouse (Fig. 2C–D). When these tumors were assessed by qPCR for the relative presence within each of non-recombined *Bcl2-fl* versus recombined *Bcl2-Δ*, very few tumors had truly developed from $Bcl2^{\Delta/\Delta}$ cells (Fig. 2E–F). Notably, these few tumors arose at an even longer latency than suggested by the germline genotype group delay of 8 weeks. Histology of these tumors continued to reflect morphology and immunohistochemical staining consistent with human synovial sarcoma and $hSS2;Bcl2^{wt/wt}$ mouse tumors (Fig. 2G), with the exception that no biphasic tumors were observed in the $hSS2;Bcl2^{fl/fl}$ tumors (Fig. 2H). Immunoblotting in $hSS2;Bcl2^{fl/fl}$ tumors revealed a loss of BCL2 at the protein level in only the tumors homozygous for recombined $Bcl2^{\Delta}$ alleles (Fig. 2I).

Pharmacologic inhibition of BCL2 minimally impacts synovial sarcoma

We previously demonstrated some efficacy with the pan-BCL2/BCLxL/BCLw inhibitor navitoclax (ABT-263) against human SS cell lines *in vitro* and mouse SSs *in vivo*. In contrast, the more BCL2-specific inhibitor, ABT-199 exhibited weak potency in SS *in vitro* assays looking at cell viability (Fig. 3A–B). We hypothesized that despite the lack of potency *in vitro*, BCL2i could sensitize human SS cell lines to the chemotherapeutic agent doxorubicin. However, the combined treatment of ABT-199 and doxorubicin showed minimal synergy and only at very high concentrations of ABT-199 (Fig. 3C). These observations were recapitulated *in vivo*. Mouse tumor treatments with ABT-199 and vehicle showed metabolic progression while subtle metabolic response was observed with doxorubicin (Fig. 3D–E), which mimics clinical observations.

Pharmacologic inhibition of BCLxL impacts synovial sarcoma

The previously reported effects of ABT-263 could be explained by its combined targeting of BCLxL and BCLw in addition to BCL2. Immunoblot analysis of 5 different human SS cell lines revealed that BCLxL is expressed at moderate levels (Fig. 3F). To address whether BCLxL is a suitable drug target in SS, we tested the potency of a BCLxL specific inhibitor, BXI-72, in cell viability assays *in vitro* (Fig. 3A). BCLxL inhibition was 20 times more potent than ABT-199, inducing cell death with an IC_{50} of < 750 nM across three different human SS cell lines (Fig. 3B). We next assessed the efficacy of BXI-72 in *in vivo* experiments. In a previous report using BXI-72 *in vivo*, Park et al. demonstrated a significant reduction in tumor masses, but within a very small therapeutic window. After starting with 30 mg/kg, we reverted to 20 mg/kg to avoid treatment related toxicities. Even at the lower dose of 20 mg/kg, we measured >50% reduction in tumor volume after 7 days of treatment (Fig. 3G). Extracted tumors demonstrated large necrotic areas histologically and upregulation of BID, a proapoptotic protein, as detected by immunoblotting (Fig. 3H–I), suggesting a targetable approach in synovial sarcoma.

Discussion

We have previously shown that *Bcl2* expression was activated in mouse embryonic fibroblasts (MEFs) induced to express *SS18-SSX*, and that *BCL2/Bcl2* expression was reduced upon knock-down of *SS18-SSX* fusions in human and mouse SS cell lines (9). Interestingly, even with the increased expression of *Bcl2*, MEFs expressing *SS18-SSX* nonetheless underwent apoptosis. This may relate to the fact that many BCL2 family members, both anti- and pro-apoptosis in character are direct targets of transcriptional activation by SS18-SSX.

While the transcriptional activation of *Bcl2* is insufficient to prevent apoptosis in mouse embryonic fibroblasts, induced overexpression of *Bcl2* clearly enhanced synovial sarcomagenesis in mice. While the preliminary observations of the group-delineated Kaplan-Meier plots for the tumor-free fraction suggested minimal impact of *Bcl2* genetic disruption, careful assessment of the tumors arising in this group demonstrated that very few of the tumors had developed following biallelic Cre-mediated silencing of *Bcl2*. That two tumors developed in this somatic genetic scenario with demonstrable Cre-mediated recombination of both *Bcl2* alleles and the absence of BCL2 protein in tumor cells by immunohistochemistry proves that BCL2 is not strictly required for SS18-SSX2-mediated sarcomagenesis. Nonetheless, the upregulation of *Bcl2* plays a significant—even if not completely necessary—role in synovial sarcomagenesis. The association of synovial sarcomas with increased familial risk for BCL2-related malignancies in lymphoma and CLL suggested that some propensity to overexpress BCL2 might associate with higher rates of completing transformation in cells that begin expressing an SS18-SSX fusion oncogene in humans as well.

A clear distinction must be made between a role for BCL2 in synovial sarcomagenesis, and its role in maintenance of fully transformed SS cells or tumors. Importantly, we and others have noted previously that knock-down of *BCL2/Bcl2* in human and mouse SS cell lines had no apparent impact on their survival or proliferation alone (9). Because ABT-199 is such a potent inhibitor of BCL2, we anticipated that it would provide a more robust inhibition of the pathway than siRNA knock-down of the transcript. Nonetheless, ABT-199 failed to deliver the relatively dramatic results of the less BCL2-specific ABT-263, tested previously in SS cell lines (9). Even with doxorubicin, ABT-199 demonstrated minimal synergy. Only 1 tumor in the mice tested demonstrated a modest response, similar to administration of doxorubicin as a separate single agent. We therefore must reluctantly conclude that BCL2 is less critical to the maintenance of cell health in SS cancer cells than it is to the early stages of synovial sarcomagenesis. BCL2 alone is therefore not a therapeutic target in SS.

Alternatively, BCLxL may be a therapeutic target in SS. BCLxL is present in cell lines at the protein level. BCLxL is expressed in human tumors at the transcript level, but not as dramatically as is BCL2 itself. We have shown that SS is heavily primed toward apoptosis, by the expression of many pro-apoptotic effector proteins. We have also shown that specific mitochondrial anti-apoptosis proteins are specifically downregulated in SS (MCL1 and BCL2A1) (9). We have considered in the past that more BCL2 was the counterbalance to

this. It may be that the mitochondrial anti-apoptosis node, including BCL2 and BCLxL are both active, but that BCLxL is more easily poisoned.

Pharmacologic agents that demonstrate efficacy against spontaneously developing tumors that arise from genetic induction have passed a much higher bar than efficacy against cell lines in culture or xenografted into immunocompromised mouse flanks. We have tested many drugs in our mouse models after demonstrable efficacy *in vitro*, finding their efficacy to be similarly disappointing to the typical application of drugs in human SS patients. Doxorubicin, which rather effectively kills most SS cell lines in a culture dish, but demonstrates only subtle cytoreduction in a minority of human SS patients, had similar response rates in the mouse model, albeit the metabolic activity was significantly reduced. That BXI-72 demonstrated actual cytoreduction argues for its potential as an agent against SS. As its clinical development progresses, SS may be a wise group for focus.

Supplementary Material

Refer to Web version on PubMed Central for supplementary material.

Acknowledgments

The work presented was directly supported by a Damon Runyon Cancer Research Foundation Clinical Investigator Award and the Paul Nabil Bustany Memorial Fund for Synovial Sarcoma Research. Additional support was received from R01CA201396, P30CA042014, 2R01CA136534 and 1U54CA168512-01 from the National Cancer Institute and the Huntsman Research Foundation. The authors gratefully received histology technical assistance from Sheryl Tripp at ARUP laboratories and Huntsman Cancer histology core.

References

1. Herzog CE. Overview of sarcomas in the adolescent and young adult population. J Pediatr Hematol Oncol. 2005; 27(4):215–8. [PubMed: 15838394]
2. Krieg AH, Hefti F, Speth BM, Jundt G, Guillou L, Exner UG, von Hochstetter AR, Cserhati MD, Fuchs B, Mouhsine E, Kaelin A, Klenke FM, Siebenrock KA. Synovial sarcomas usually metastasize after >5 years: a multicenter retrospective analysis with minimum follow-up of 10 years for survivors. Ann Oncol. 2011; 22(2):458–67. DOI: 10.1093/annonc/mdq394 [PubMed: 20716627]
3. Eilber FC, Brennan MF, Eilber FR, Eckardt JJ, Grobmyer SR, Riedel E, Forscher C, Maki RG, Singer S. Chemotherapy is associated with improved survival in adult patients with primary extremity synovial sarcoma. Ann Surg. 2007; 246(1):105–13. DOI: 10.1097/01.sla.0000262787.88639.2b [PubMed: 17592298]
4. Karavasilis V, Seddon BM, Ashley S, Al-Muderis O, Fisher C, Judson I. Significant clinical benefit of first-line palliative chemotherapy in advanced soft-tissue sarcoma: retrospective analysis and identification of prognostic factors in 488 patients. Cancer. 2008; 112(7):1585–91. DOI: 10.1002/cncr.23332 [PubMed: 18278813]
5. Clark J, Rocques PJ, Crew AJ, Gill S, Shipley J, Chan AM, Gusterson BA, Cooper CS. Identification of novel genes, SYT and SSX, involved in the t(X;18)(p11.2;q11.2) translocation found in human synovial sarcoma. Nat Genet. 1994; 7(4):502–8. DOI: 10.1038/ng0894-502 [PubMed: 7951320]
6. Su L, Sampaio AV, Jones KB, Pacheco M, Goytain A, Lin S, Poulin N, Yi L, Rossi FM, Kast J, Capecchi MR, Underhill TM, Nielsen TO. Deconstruction of the SS18-SSX fusion oncoprotein complex: insights into disease etiology and therapeutics. Cancer Cell. 2012; 21(3):333–47. DOI: 10.1016/j.ccr.2012.01.010 [PubMed: 22439931]

7. Kadoch C, Crabtree GR. Reversible disruption of mSWI/SNF (BAF) complexes by the SS18-SSX oncogenic fusion in synovial sarcoma. Cell. 2013; 153(1):71–85. DOI: 10.1016/j.cell.2013.02.036 [PubMed: 23540691]
8. Hirakawa N, Naka T, Yamamoto I, Fukuda T, Tsuneyoshi M. Overexpression of bcl-2 protein in synovial sarcoma: a comparative study of other soft tissue spindle cell sarcomas and an additional analysis by fluorescence in situ hybridization. Hum Pathol. 1996; 27(10):1060–5. [PubMed: 8892591]
9. Jones KB, Su L, Jin H, Lenz C, Randall RL, Underhill TM, Nielsen TO, Sharma S, Capecchi MR. SS18-SSX2 and the mitochondrial apoptosis pathway in mouse and human synovial sarcomas. Oncogene. 2013; 32(18):2365–71. 75, e1–5. DOI: 10.1038/onc.2012.247 [PubMed: 22797074]
10. Hata AN, Engelman JA, Faber AC. The BCL2 Family: Key Mediators of the Apoptotic Response to Targeted Anticancer Therapeutics. Cancer Discov. 2015; 5(5):475–87. DOI: 10.1158/2159-8290.CD-15-0011 [PubMed: 25895919]
11. Gandhi L, Camidge DR, Ribeiro de Oliveira M, Bonomi P, Gandara D, Khaira D, Hann CL, McKeegan EM, Litvinovich E, Hemken PM, Dive C, Enschede SH, Nolan C, Chiu YL, Busman T, Xiong H, Krivoshik AP, Humerickhouse R, Shapiro GI, Rudin CM. Phase I study of Navitoclax (ABT-263), a novel Bcl-2 family inhibitor, in patients with small-cell lung cancer and other solid tumors. J Clin Oncol. 2011; 29(7):909–16. DOI: 10.1200/JCO.2010.31.6208 [PubMed: 21282543]
12. Roberts AW, Davids MS, Pagel JM, Kahl BS, Puvvada SD, Gerecitano JF, Kipps TJ, Anderson MA, Brown JR, Gressick L, Wong S, Dunbar M, Zhu M, Desai MB, Cerri E, Heitner Enschede S, Humerickhouse RA, Wierda WG, Seymour JF. Targeting BCL2 with Venetoclax in Relapsed Chronic Lymphocytic Leukemia. N Engl J Med. 2016; 374(4):311–22. DOI: 10.1056/NEJMoa1513257 [PubMed: 26639348]
13. Konopleva M, Pollyea DA, Potluri J, Chyla B, Hogdal L, Busman T, McKeegan E, Salem AH, Zhu M, Ricker JL, Blum W, DiNardo CD, Kadia T, Dunbar M, Kirby R, Falotico N, Leverson J, Humerickhouse R, Mabry M, Stone R, Kantarjian H, Letai A. Efficacy and Biological Correlates of Response in a Phase II Study of Venetoclax Monotherapy in Patients with Acute Myelogenous Leukemia. Cancer Discov. 2016; 6(10):1106–17. DOI: 10.1158/2159-8290.CD-16-0313 [PubMed: 27520294]
14. Park D, Magis AT, Li R, Owonikoko TK, Sica GL, Sun SY, Ramalingam SS, Khuri FR, Curran WJ, Deng X. Novel small-molecule inhibitors of Bcl-XL to treat lung cancer. Cancer Res. 2013; 73(17):5485–96. DOI: 10.1158/0008-5472.CAN-12-2272 [PubMed: 23824742]
15. Agresti A, Min Y. Simple improved confidence intervals for comparing matched proportions. Stat Med. 2005; 24(5):729–40. DOI: 10.1002/sim.1781 [PubMed: 15696504]
16. Kawai A, Naito N, Yoshida A, Morimoto Y, Ouchida M, Shimizu K, Beppu Y. Establishment and characterization of a biphasic synovial sarcoma cell line, SYO-1. Cancer Lett. 2004; 204(1):105–13. [PubMed: 14744540]
17. Nojima T, Wang YS, Abe S, Matsuno T, Yamawaki S, Nagashima K. Morphological and cytogenetic studies of a human synovial sarcoma xenotransplanted into nude mice. Acta Pathol Jpn. 1990; 40(7):486–93. [PubMed: 2171298]
18. Naka N, Takenaka S, Araki N, Miwa T, Hashimoto N, Yoshioka K, Joyama S, Hamada K, Tsukamoto Y, Tomita Y, Ueda T, Yoshikawa H, Itoh K. Synovial sarcoma is a stem cell malignancy. Stem Cells. 2010; 28(7):1119–31. DOI: 10.1002/stem.452 [PubMed: 20518020]
19. Barrott JJ, Illum BE, Jin H, Zhu JF, Mosbruger T, Monument MJ, Smith-Fry K, Cable MG, Wang Y, Grossmann AH, Capecchi MR, Jones KB. beta-catenin stabilization enhances SS18-SSX2-driven synovial sarcomagenesis and blocks the mesenchymal to epithelial transition. Oncotarget. 2015; 6(26):22758–66. DOI: 10.18632/oncotarget.4283 [PubMed: 26259251]
20. Prichard MN, Prichard LE, Baguley WA, Nassiri MR, Shipman C Jr. Three-dimensional analysis of the synergistic cytotoxicity of ganciclovir and zidovudine. Antimicrob Agents Chemother. 1991; 35(6):1060–5. [PubMed: 1929243]

Implications

The association of BCL2 expression with synovial sarcoma is found to fit with a subtle, but significant impact of its enhanced presence or absence during early tumorigenesis. However, specific pharmacological inhibition of BCL2 does not demonstrate a persistent dependence in fully developed tumors. Conversely, inhibition of the BCL2 family member, BCLxL, resulted in nanomolar potency against human synovial sarcoma cell lines and 50% tumor reduction in a genetically engineered mouse (GEM) model.

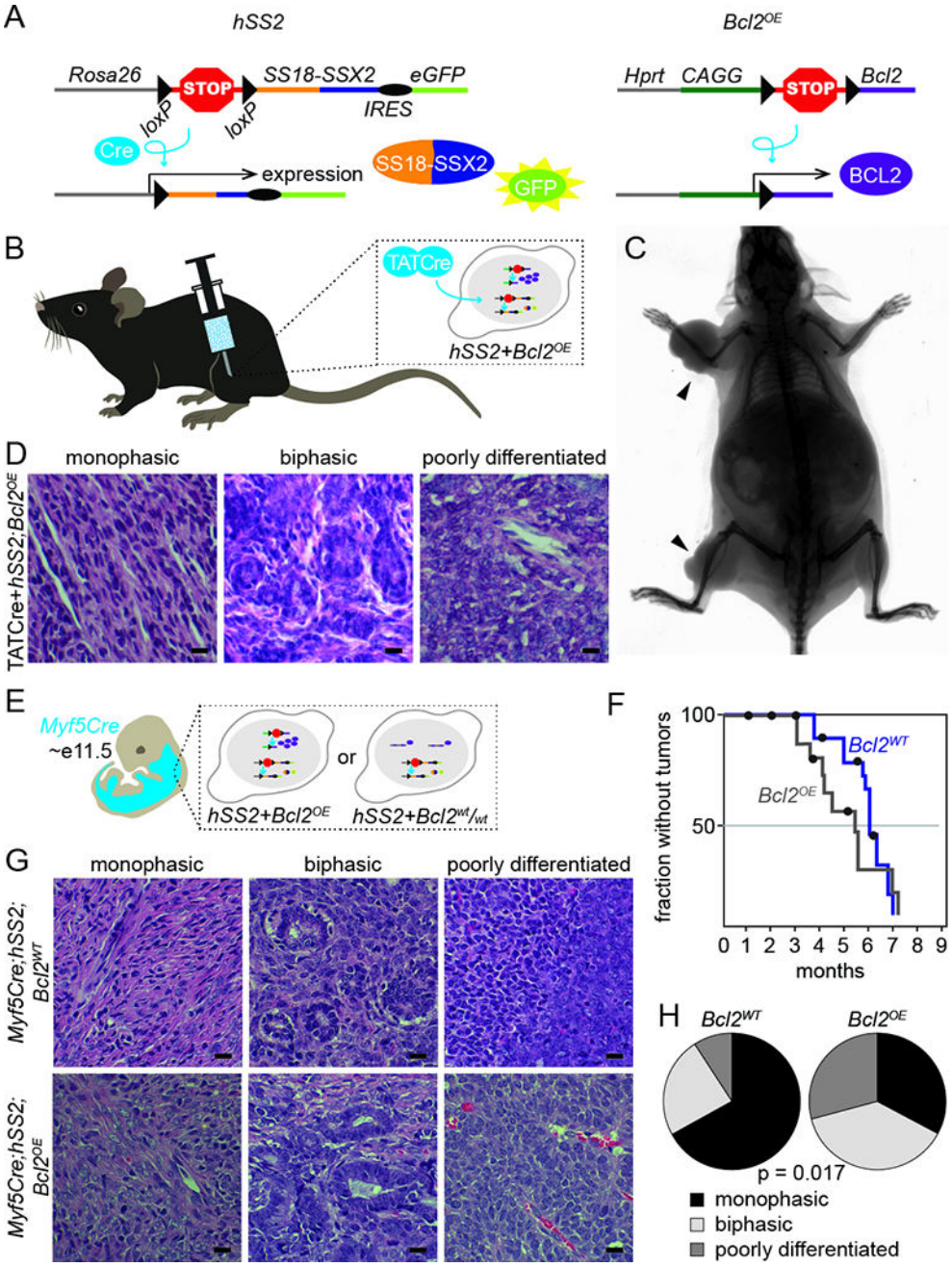

Figure 1. Bcl2 overexpression in synovial sarcoma enhances sarcomagenesis

A. Schematic of alleles for *SS18-SSX2* and *Bcl2* overexpression with their respective recombination products (IRES, internal ribosomal entry site).

B. Schematic of TATCre injection technique resulting in the combinatorial expression of *hSS2* and *Bcl2*.

C. Radiograph image of *hSS2;Bcl2*^{OE} mouse 8 months post TATCre injection in the right forearm and right hindlimb (black arrow).

D. Photomicrographs of H&E histology examples of monophasic, biphasic, and poorly differentiated synovial sarcomas from *hSS2;Bcl2*^{OE} mice induced with TATCre.

E. Schematic of *Myf5Cre+* distribution in E11.5 embryo resulting in the expression of *hSS2* or *hSS2;Bcl2*^{OE} during embryogenesis.

F. Kaplan-Meier plot of the nonmorbid fraction of *hSS2;Bcl2*^{OE} (gray) and *hSS2;Bcl2*^{WT} (blue) induced in *Myf5Cre+* mice. Statistical difference (Log-rank test) between *hSS2;Bcl2*^{OE} and *hSS2;Bcl2*^{WT}, p value = 0.023.

G. Photomicrographs of H&E histology examples of monophasic, biphasic, and poorly differentiated synovial sarcomas from *hSS2;Bcl2*^{WT} and *hSS2;Bcl2*^{OE}, mice induced in *Myf5Cre+* cells.

H. Fraction of monophasic, biphasic, and poorly differentiated histologies in *Myf5Cre;hSS2;Bcl2*^{WT} and *Myf5Cre;hSS2;Bcl2*^{OE}, mice.

(All magnification bars = 10 μm)

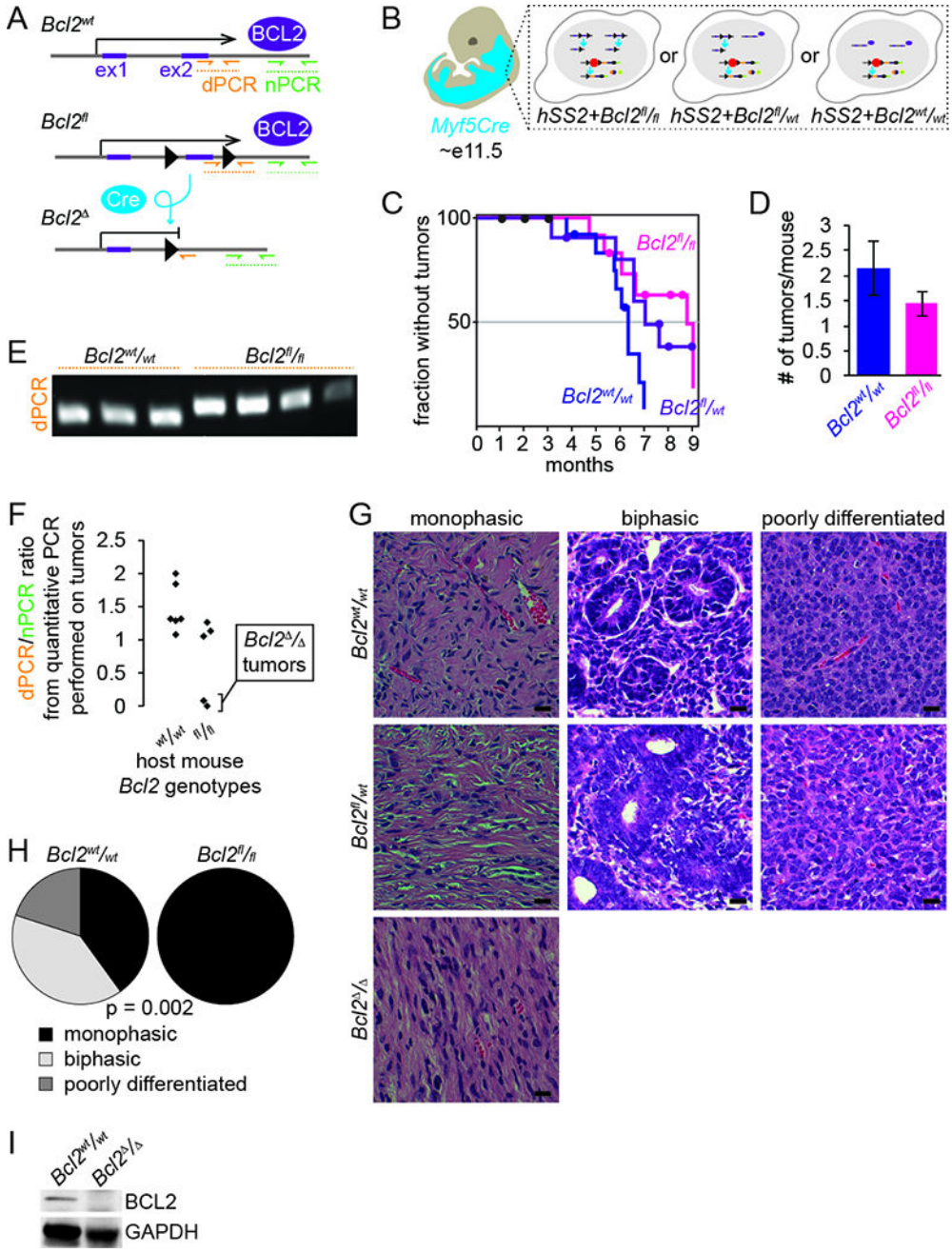

Figure 2. Bcl2 conditional deletion in synovial sarcoma mildly disrupts sarcomagenesis

A. Schematic of alleles for *Bcl2*$^{fl/fl}$ with its respective recombination product. Also demonstrating the location of primers for detection of the recombined allele (dPCR) and the primers for normalization (nPCR).

B. Schematic of *Myf5Cre+* distribution in E11.5 embryo resulting in the expression of *hSS2* or *hSS2;Bcl2*$^{fl/fl}$ during embryogenesis.

C. Kaplan-Meier plot of the nonmorbid fraction of *hSS2;Bcl2*$^{fl/fl}$ (pink), *hSS2;Bcl2*$^{fl/wt}$ (purple) and *hSS2;Bcl2*^{WT} (blue) induced in *Myf5Cre+* mice. Statistical difference (Log-rank test) between *hSS2;Bcl2*$^{fl/fl}$ and *hSS2;Bcl2*^{WT}, p value = 0.03.

D. Graph depicting the average number of tumors per mouse between *hSS2;Bcl2$^{fl/fl}$* and *hSS2;Bcl2^{WT}*, genotypes (p value = 0.34).
E. PCR detection of the recombined *Bcl2$^{fl/fl}$* allele compared to wildtype.
F. Quantification of the recombined *Bcl2$^{fl/fl}$* allele normalized to adjacent primers, demonstrating that not all *Bcl2$^{fl/fl}$* tumors recombined to delete *Bcl2*.
G. Photomicrographs of H&E histology examples of monophasic, biphasic, and poorly differentiated synovial sarcomas from *hSS2;Bcl2^{WT}hSS2;Bcl2$^{fl/wt}$* and *hSS2;Bcl2$^{fl/fl}$* mice induced in *Myf5Cre+* cells.
H. Fraction of monophasic, biphasic, and poorly differentiated histologies in *Myf5Cre;hSS2;Bcl2^{WT}* and *Myf5Cre;hSS2;Bcl2$^{fl/fl}$* mice.
I. Immunoblots detecting the absence of BCL2 in fully recombined tumors following TATCre injection from *hSS2;Bcl2$^{fl/fl}$* mice compared to tumors from *hSS2;Bcl2^{WT}* mice. (All magnification bars = 10 μm)

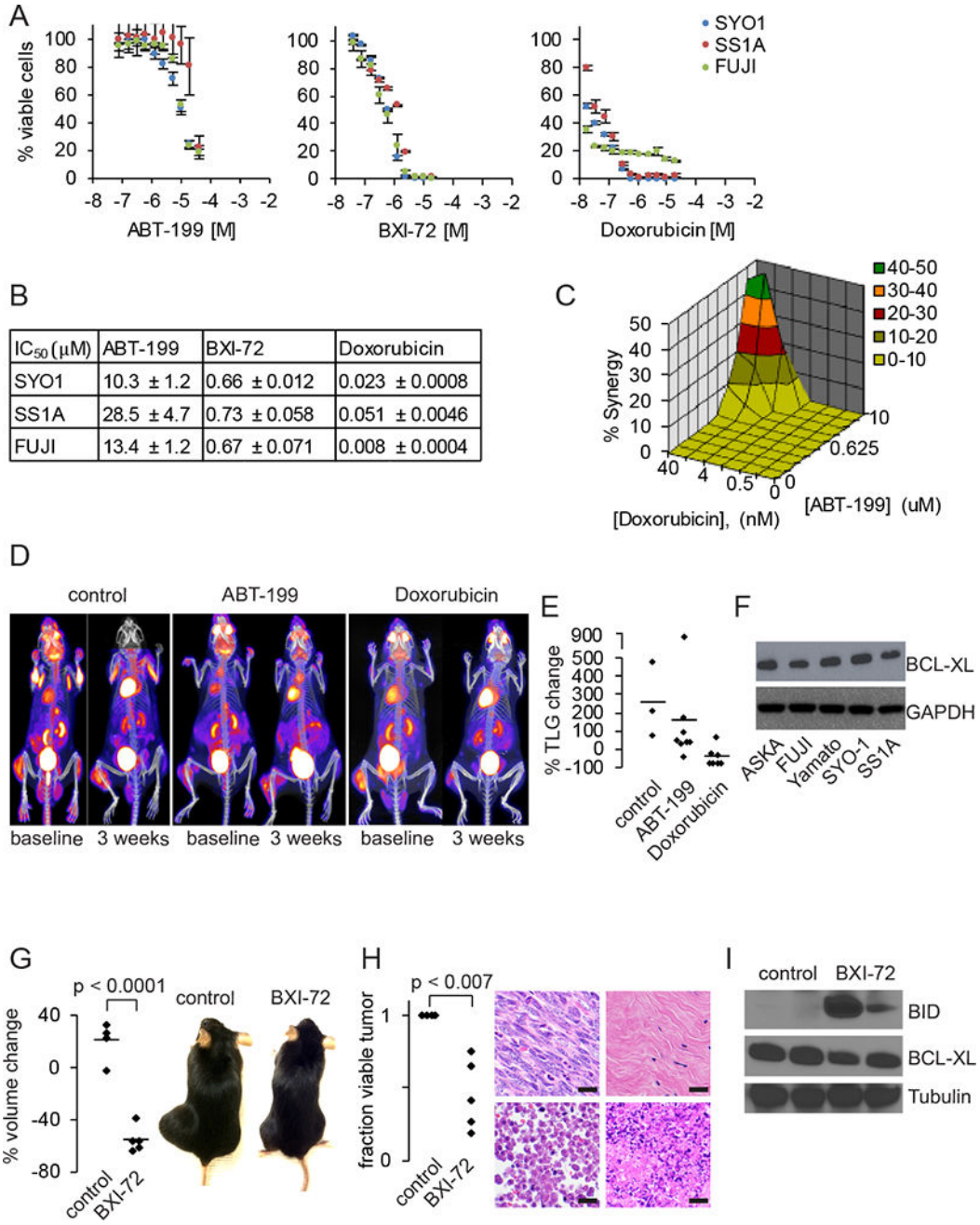

IC_{50} (μM)	ABT-199	BXI-72	Doxorubicin
SYO1	10.3 ± 1.2	0.66 ± 0.012	0.023 ± 0.0008
SS1A	28.5 ± 4.7	0.73 ± 0.058	0.051 ± 0.0046
FUJI	13.4 ± 1.2	0.67 ± 0.071	0.008 ± 0.0004

Figure 3. Targeting BCL2 and BCLxL in synovial sarcoma

A. Cell viability curves for ABT-199, BXI-72 and doxorubicin in SYO-1 (blue), SS1A (red) and FUJI (green) after 48 hours of treatment.

B. IC_{50} data for ABT-199, BXI-72 and doxorubicin in SYO-1, SS1A and doxorubicin (± SEM).

C. Mac Synergy plot between doxorubicin and ABT-199 demonstrating minimal synergy (< 50% synergy) after 72 hours of treatment.

D. FDG-PET/CT image of *Pten*$^{fl/fl}$;*hSS2* mice treated with control, ABT-199 or doxorubicin.

E. Graph of percent change in total lesion glycolysis (TLG) for synovial sarcomas treated with control, ABT-199 or doxorubicin.

F. Immunoblotting for BCLxL across five human synovial sarcoma cell lines with GAPDH as a loading control.

G. Graph depicting percent volume changes after 7 days of 20 mg/kg BXI-72 in *Pten*$^{fl/fl}$;*hSS2* mice induced with local injection of TATCre and example gross photographs of *Pten*$^{fl/fl}$;*hSS2* mice with synovial sarcomas on the left hindlimb treated with control DMSO or 20 mg/kg BXI-72.

H. Graph depicting percent necrosis in synovial sarcomas treated with control DMSO or BXI-72. Example H&E photomicrographs of necrosis identified in tumors treated with control DMSO or BXI-72: top left is viable tumor from control; top right is replacement of tumor with fibrosis in BXI-72 treated mice; bottom left is necrosis by ghost cells (anucleate); bottom right is necrosis/apoptosis by fragmentation.

I. Immunoblotting for BID (pro-apoptosis), BCLxL and tubulin in extracted synovial sarcomas treated with DMSO or BXI-72.

(All magnification bars = 10 μm)

Table 1

Relative Risk for BCL2-associated malignancies in relatives of 68 synovial sarcoma cases

Relative	n	obs/exp	RR	p	95% CI
First-degree	464	6/3.03	1.98	0.087	0.73, 4.31
Second-degree	1,348	18/9.0	2.00	0.0066	1.18, 3.16
Third-degree	3,423	28/19.1	1.46	0.0506	0.97, 2.12